

# Computational design of RNA-based oscillatory circuits

J. Binysh

\* *University of Warwick, Complexity Department*

**Abstract**—genetic circuitry, RNA's offers an attractive alternative to more traditional methods, which typically involve using proteins to regulate DNA transcription. In comparison to proteins, it is relatively straightforward

## I. INTRODUCTION

The process of gene expression can be briefly summarised as: DNA is read, and a copy of it is made, in the form of an RNA molecule (this is called *transcription*). This RNA molecule (known as messenger RNA, or mRNA) makes its way to a piece of cellular machinery called the Ribosome, which reads it, and makes a protein - which protein is made depends on the DNA sequence originally read (*translation*).

The path from genetic transcription to protein expression is naturally regulated in many ways [?]. This regulation allows the cell to control protein expression, and so cell behaviour, in response to various environmental cues. The natural cell machinery which performs this regulation offers rich possibilities for modification, and an important goal within synthetic biology is to understand and manipulate it.

As well as acting as the intermediate between DNA and protein, RNA molecules play direct and important roles in regulating cell behaviour [1]. For the synthetic biologist looking to engineer regulation of genetic circuitry, RNA's offers an attractive alternative to more traditional methods, which typically involve using proteins to regulate DNA transcription. In comparison to proteins, it is relatively straightforward to predict the structure and function of an RNA from its sequence using physiochemical models. Recently, this has been exploited to computationally design DNA sequences encoding synthetic sRNA's - small RNA's which do not code for a protein, but rather have some direct regulatory function - with regulatory behaviour that can be predicted [2] [3].

This report will focus on one such system, introduced in [3]. It will extend existing understanding of the system beyond the qualitative, by proposing a quantitative model of gene expression, in the form of a set of ODE's, and fitting it to available time series data to estimate the model's unknown parameters.

The report is structured as follows. In the remainder of this section we review the sRNA regulatory system we will consider, and discuss recent single cell fluorescence experiments performed on this system. In section II we propose a set of ODE's to model the system, and estimate its unknown parameters by fitting to time series data. Finally, in section III, we conclude, and suggest directions for further work.

## A. The sRNA regulatory system

In bacteria, one mechanism by which gene expression is regulated is as follows [4]: In order for a bacterial mRNA to be translated into a protein, the Ribosome must initially bind to the mRNA (Fig. 2). This occurs at the Ribosome Binding Site (RBS) [5], a specific nucleotide sequence found on the mRNA. In an mRNA there is an untranslated region of nucleotides at the 5' end of the molecule (the UTR), upstream of the RBS. Translation may be self repressed by this 'tail' of the mRNA folding over and binding across the RBS, forming a stem loop in the mRNA and preventing the Ribosome from binding (Fig. 2). This self repression may be released with an sRNA which binds to the same region on the mRNA - the new conformation of the sRNA:mRNA complex uncovers the RBS, allowing the Ribosome to bind. In summary, the presence of the sRNA positively regulates gene expression.

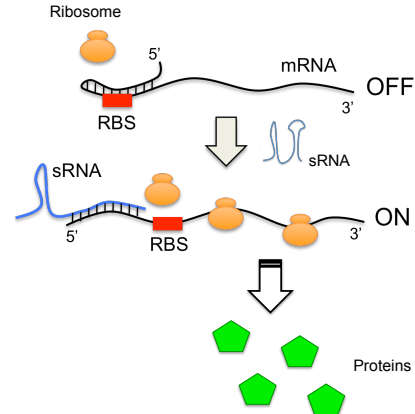


Fig. 2. A mechanism by which sRNA's can regulate gene expression. Initially, the 5' UTR of the mRNA is folded over the RBS, forming a loop and blocking Ribosome binding. The sRNA binds to this mRNA, causing a conformational change which uncovers the RBS, and allows translation to occur. Image reproduced from [3]

[3] proposed a computational methodology to design general genetic circuits based on RNA interactions, and as a case study of the methodology chose to design a synthetic sRNA- mRNA pair capable of acting in the manner described above. The algorithm assumed an interaction scheme between the RNA's as shown in Fig. 7. The two RNA's, originally in their own individually folded states, would initially interact via a small 'toehold' sequence of unpaired nucleotides to form an unstable transition state. This intermediate complex would

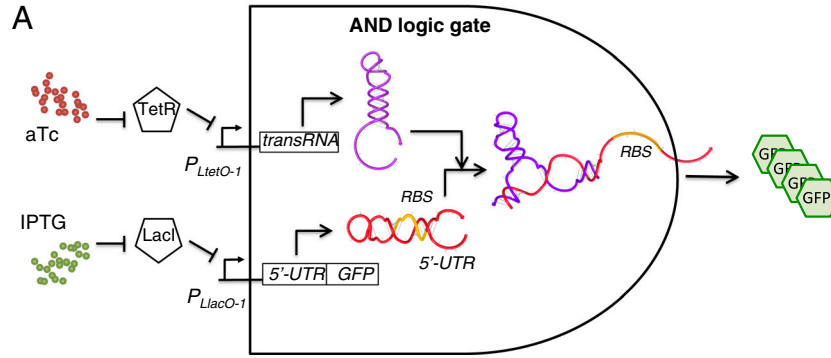


Fig. 1. A logical AND gate formed from a self repressed mRNA, and an sRNA which uncovers its RBS. In this system, transcription of the sRNA (transRNA) and mRNA (5'-UTR.GFP) are controlled by two promoter regions,  $P_{LtetO-1}$  and  $P_{LlacO-1}$ . These are disabled by the presence of two chemical repressors, TetR and LacI, found naturally in the strain of *E. coli* discussed. These chemical repressors are themselves disabled by two chemicals, aTC and IPTG. In the notation of the diagram, a barred line indicates repression, and an arrowed line indicates production. We see a 'double negative' in aTC repressing TetR, which itself represses transcription of the sRNA (likewise for IPTG and the mRNA). Thus presence of the sRNA and mRNA are controlled by the presence of aTC and IPTG, which can be experimentally introduced to the cell. Image reproduced from [3].

then rapidly form a final, stable complex with the desired conformation. By suggesting sRNA and mRNA sequences which optimised this energy landscape, [3] suggested several devices which would form a stable hybrid with the RBS free, and experimentally validated their function in *E. coli*, using an mRNA which codes for GFP for experimental ease (note the algorithm only optimises the 5' UTR of the mRNA, so the actual protein being coded for is unimportant).

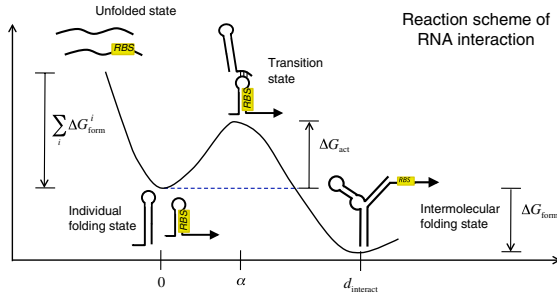


Fig. 3. A network with an intuitively clear community structure, which is captured by the partition chosen, shown in gray. Image reproduced from [3]

Further, by placing the concentrations of the sRNA and mRNA under the control of tuneable promoters, [3] constructs a logical AND gate from one of the proposed devices (RAJ11) *in vivo* (Fig. 1). In this system, transcription of the designed sRNA and mRNA are placed under the control of promoter regions,  $P_{LtetO-1}$  and  $P_{LlacO-1}$  [6]. These are in turn controlled by two transcriptional repressors, TetR and LacI, which are naturally present in the strain of *E. coli* considered. These repressors disable the promoter regions, and so by default transcription of the RNA's is turned off, and no protein is

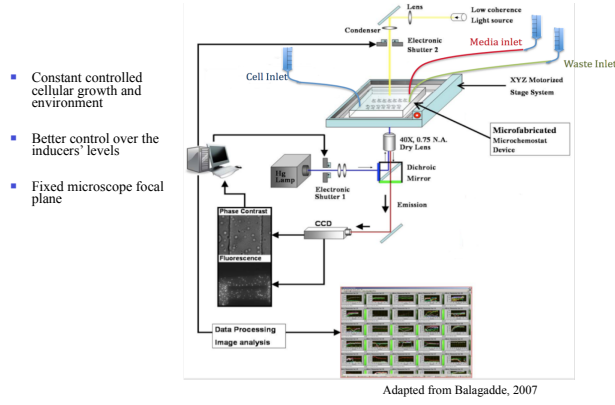
produced. These repressors can themselves be disabled by the presence of two chemicals, aTC and IPTG, which can be introduced externally into the cell (Fig. 1). So transcription of the two RNA's is indirectly controlled by the presence of two chemicals - if neither is present, sRNA and mRNA transcription is repressed, and no protein is produced. If only one is present, the AND gate remains off, either because there is no mRNA to be translated into protein, or because the mRNA is self repressed. But when both are present, the conformational change discussed above occurs, and protein is produced.

promoter?

Although a qualitative understanding of this system exists [3], it is of interest to attempt a quantitative understanding of the genetic circuit involved. Such an understanding would allow, for example, tailoring of the system in response to design requirements, by altering the values of the important parameters of the model. By changing which sRNA-mRNA device is used in the system, it would also allow exploration of the relationship between the thermodynamic properties of each device, and the model's rate constants.

## B. Single Cell Fluorescence Data

Recent experiments have used timelapse microscopy to observe bacteria as they are periodically forced with a varying aTC or IPTG concentration [7]. The bacteria are grown a single layer thick in rows of chambers. A medium constantly flows through these chambers, allowing normal feeding of the bacteria, and the introduction of aTC or IPTG. The chambers are monitored with software which traces the position of each cell over time, allowing timeseries of individual cell fluorescences to be recorded.



Growing cells in single layers with microfluidics

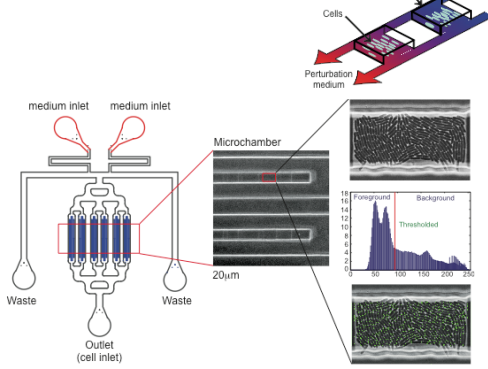


Fig. 4. A schematic of an experimental setup which allows single cell fluorescences to be recorded over time. Bacteria are grown in chambers, with a constant supply of medium flowing through them from the media inlet. This inlet also allows the introduction of aTc IPTG. Software then traces these cells, allowing fluorescence timeseries to be built. Image reproduced from [7].

The data we will consider consists of three sets of individual cell timeseries, labelled *13\_9*, *14\_7* and *14\_9*. They correspond to three different experimental runs of the above apparatus, for which IPTG concentration was held constant, at a value assumed large enough to saturate the cell's response, and aTc concentrations were changed with varying periods. Section A shows the full datasets, with their forcing functions.

## II. RESULTS AND DISCUSSION

### A. Model Derivation

We propose a simple model, consisting of a set of ODE's with mass action kinetics [?], to describe the system. Tables I, II give complete descriptions of the parameters and state variables.

$$\begin{aligned} \frac{ds}{dt} &= \frac{N\alpha_T}{f_T} y(t) - (\mu + \delta_s)s - k_{on}sm + k_{off}s : m \quad (1) \\ \frac{dm}{dt} &= \frac{N\alpha_L}{f_L} x(t) - (\mu + \delta_m)m - k_{on}sm + k_{off}s : m \quad (2) \end{aligned}$$

$$\frac{ds : m}{dt} = k_{on}sm - (k_{off} + k_{hyb})s : m - (\mu + \delta_{sm})s : m \quad (3)$$

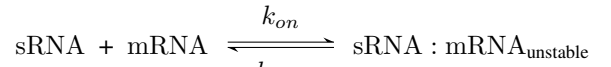
$$\frac{dc}{dt} = k_{hyb}s : m - (\mu + \delta_c)c \quad (4)$$

$$\frac{dp}{dt} = \beta m + f_s \beta c - (\gamma + \mu + \delta_g)p - \frac{v_z p}{K_z + p + g} \quad (5)$$

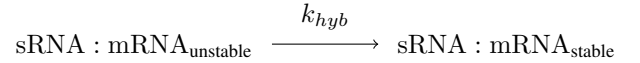
$$\frac{dg}{dt} = \gamma p - (\mu + \delta_g)g - \frac{v_z g}{K_z + p + g} \quad (6)$$

$$z = z_0 + \frac{g}{\theta} \quad (7)$$

Based on the reaction mechanism in Fig. 7, the hybridization of the sRNA and mRNA first into an unstable complex, then a stable one, is modelled in eqs.1 - 4. The initial binding is modelled as a reversible reaction with forward and backward rates  $k_{on}$  and  $k_{off}$ .



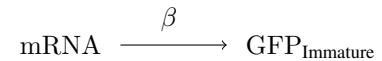
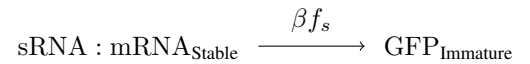
after which the stabilization  $k_{hyb}$  is modelled as an irreversible reaction with rate  $k_{hyb}$ .



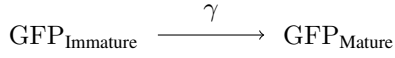
In addition, these complexes are given degradation rates,  $\delta_s$ ,  $\delta_m$ ,  $\delta_{sm}$ ,  $\delta_c$ , and dilution of chemical concentrations due to cell growth are modelled with a dilution rate  $\mu$ .

Control of the system by aTc and IPTG is modelled by  $y(t)$  and  $x(t)$  in eqs.1-2.  $y(t)$  models the response of the sRNA transcription rate to a time varying aTc concentration - it is normalised to lie between 1 and  $f_T$ , and is typically sigmoid in response to aTc concentration [3]. Thus the forcing may vary between  $N \frac{1}{f_T}$  and  $N \frac{\alpha_T}{f}$ , where  $\alpha_T$  is the maximal transcription rate of the  $P_{LtetO-1}$  promoter. When engineering the system, many copies of the  $P_{LtetO-1}$  promoter and section of DNA coding for sRNA may be placed in the plasmid DNA - this is modelled by the copy number,  $N$ . Identical considerations hold for  $x(t)$  and IPTG concentrations.

We explicitly model translation as a simple one step process in eqs. 5-7. There is a small rate of translation of the self repressed mRNA [3], which is modelled at rate  $\beta$ , and a larger one for translation of the stable complex,  $\beta f_s$ . Here  $f_s$  represents the fractional change in translation rate between the repressed mRNA and the unrepressed complex.



Initially, the translated GFP is in an immature state, and will not fluoresce. To account for this, we include a maturation rate,  $\gamma$



Degradation of the immature and mature GFP is modelled in two ways. Firstly a generic degradation rate  $\delta_g$ , assumed identical for the mature and immature species, with the dilution rate  $\mu$  shared by all species.

para about clpX

Finally, eq. 7 simply represents calibration of mature GFP levels to experimentally observed fluorescence.

TABLE I. MODEL PARAMETERS (THOSE TO BE ESTIMATED SHOWN IN BOLD)

Parameter	Units	Definition
N		Number of copies of promoter existing on plasmid DNA
$z_0$	AFU	Baseline experimental fluorescence
$\alpha_L$	nM/min	Maximal transcription rate of $P_{\text{LlacO}-1}$ promoter
$\alpha_T$	nM/min	Maximal transcription rate of $P_{\text{LtetO}-1}$ promoter
$f_L$		Unitless ratio between repressed and unrepressed $P_{\text{LlacO}-1}$ transcription rate
$f_T$		Unitless ratio between repressed and unrepressed $P_{\text{LtetO}-1}$ transcription rate
$\delta_g$	/min	GFP degradation rate
$\gamma$	/min	GFP maturation rate
$v_z$	nM/min	degradation constant of clpx
$K_z$	nM/min	Dissociation constant of clpx
$\Theta$	nM/AFU	Ratio between GFP concentration and observed fluorescence
$\mu$	/min	Dilution rate
$\delta_m$	/min	mRNA degradation rate
$\delta_s$	/min	sRNA degradation rate
$\delta_{sm}$	/min	Unstable sRNA:mRNA degradation rate
$\delta_c$	/min	Stable sRNA:mRNA degradation rate
$k_{on}$	/min	sRNA:mRNA binding rate
$k_{off}$	/min	sRNA:mRNA unbinding rate
$k_{hyb}$	/min	sRNA:mRNA hybridization rate
$\beta$	/min	Baseline translation rate of repressed mRNA
$f_s$		Ratio of repressed mRNA to unrepressed complex translation rate.

TABLE II. STATE VARIABLES

State variable	Units	Definition
$s$	nM	sRNA concentration
$m$	nM	mRNA concentration
$s : m$	nM	Unstable sRNA:mRNA complex concentration
$c$	nM	Stable sRNA:mRNA complex concentration
$p$	nM	Immature GFP concentration
$g$	nm	Mature GFP concentration
$z$	AFU	Observed fluorescence
$y(t)$		Unitless aTc forcing function
$x(t)$		Unitless IPTG forcing function

## B. Parameter Estimation

Our next goal is to estimate the unknown parameters of this model, given the available fluorescence time series data, by fitting predicted time series from the model to the data. Typically, this is done by minimising the least squares error between model prediction and the experimental data [8]–[10]. Suppose we have some ODE model of our system

$$\frac{dy}{dt} = f(y, \theta, t) \quad (8)$$

where  $y$  is our state vector,  $\theta$  is a vector of model parameters, and  $t$  is time (representing the fact that the model may have some explicit time dependence). The model may be integrated numerically, giving a prediction  $y(t, \theta)$ . An error between the model prediction and an experimental time series is defined as

$$J(\theta) = \sum_{i=1}^N (y_{\text{exp}}(t_i) - y(t_i, \theta))^2 \quad (9)$$

where the experimental timeseries,  $y_{\text{exp}}(t_i)$  is evaluated at timepoints  $t_i$ ,  $i = 1 \dots N$ . This error function defines a landscape in  $\theta$  space, and we seek to minimise it by varying  $\theta$ . In our case, we do not have experimental data on the full state vector, but only one component of it - the observed fluorescence,  $z(t)$ . In addition, rather than a single experimental run, we have many, corresponding to a timeseries from each cell. We incorporate this by fitting to the experimental mean of the data, and only minimising over the observed component. Our minimisation problem is thus

$$\min_{\theta} \sum_{i=1}^N (z_{\text{exp,mean}}(t_i) - z(t_i, \theta))^2 \quad (10)$$

The next step is performing the minimisation. In general, the landscape defined by the error function is multimodal, and may be very rugged.<sup>1</sup> A local optimisation algorithm will often get stuck in local minima. To try and surmount this problem, [9] suggests the use of a global optimisation algorithm, and in particular recommends several Evolutionary Algorithms, of which we choose one, the CMA-ES [11], [12].

In order to reduce the dimensionality of our search space, we can perform a literature search for existing values of some of our parameters, simplify our model to remove others, and place bounds on those that remain. Section A contains a list of parameter values found in the literature, where available, and their reference, as well as initial bounds placed on parameters not found in the literature. To further reduce the search space, we assume that  $\delta_m$ ,  $\delta_{sm}$  and  $\delta_c$  all take similar values, and set them equal.

After this is done, we are left with a 9 dimensional search space, bounded by a hypercube (parameters to be estimated are shown in bold in I). We begin by fitting two of the datasets, 13\_9 and 14\_7

<sup>1</sup>this is true even if ODE model is linear in its parameters, as is almost the case for us - though the ODE model is linear, the resulting solutions are in general not. A counterexample is the harmonic oscillator.

## III. CONCLUSIONS AND FURTHER WORK

## REFERENCES

- [1] F. J. Isaacs, D. J. Dwyer, and J. J. Collins, "RNA synthetic biology," *Nature biotechnology*, vol. 24, no. 5, pp. 545–554, 2006.
- [2] G. Rodrigo, T. E. Landrain, S. Shen, and A. Jaramillo, "A new frontier in synthetic biology: Automated design of small RNA devices in bacteria," pp. 529–536, 2013.
- [3] G. Rodrigo, T. E. Landrain, and A. Jaramillo, "De novo automated design of small RNA circuits for engineering synthetic riboregulation in living cells," *Proceedings of the National Academy of Sciences*, vol. 109, no. 38, pp. 15 271–15 276, 2012.
- [4] T. Soper, P. Mādin, N. Majdalani, S. Gottesman, and S. a. Woodson, "Positive regulation by small RNAs and the role of Hfq," *Proceedings of the National Academy of Sciences of the United States of America*, vol. 107, no. 21, pp. 9602–9607, 2010.
- [5] J. Shine and L. Dalgarno, "Identical 3'-terminal octanucleotide sequence in 18S ribosomal ribonucleic acid from different eukaryotes. A proposed role for this sequence in the recognition of terminator codons," *The Biochemical journal*, vol. 141, no. 3, pp. 609–615, 1974.
- [6] R. Lutz and H. Bujard, "Independent and tight regulation of transcriptional units in escherichia coli via the LacR/O, the TetR/O and AraC/I1-12 regulatory elements," *Nucleic Acids Research*, vol. 25, no. 6, pp. 1203–1210, 1997.
- [7] A. Jaramillo, "Predictive Modelling of Riboregulatory Circuits to Re-engineer Living Cells." [Online]. Available: [http://www2.warwick.ac.uk/fac/sci/wcpm/seminars/wcpm/\\_seminar/\\_presentation/\\_alfonso/\\_jaramillo.pdf](http://www2.warwick.ac.uk/fac/sci/wcpm/seminars/wcpm/_seminar/_presentation/_alfonso/_jaramillo.pdf)
- [8] D. Brewer, M. Barenco, R. Callard, M. Hubank, and J. Stark, "Fitting ordinary differential equations to short time course data," *Philosophical transactions. Series A, Mathematical, physical, and engineering sciences*, vol. 366, no. 1865, pp. 519–544, 2008.
- [9] E. Algorithms, E. Algorithms, C. G. Moles, C. G. Moles, P. Mendes, P. Mendes, J. R. Banga, and J. R. Banga, "Parameter Estimation in Biochemical Pathways: A Comparison of Global Optimization Methods," *Genome Research*, pp. 2467–2474, 2003.
- [10] C. Y. Hu, J. Varner, and J. B. Lucks, "Generating effective models and parameters for RNA genetic circuits," *ACS Synthetic Biology*, p. 150605124221004, 2015. [Online]. Available: <http://pubs.acs.org/doi/abs/10.1021/acssynbio.5b00077>
- [11] N. Hansen, "The CMA evolution strategy: A comparing review," *Studies in Fuzziness and Soft Computing*, vol. 192, no. 2006, pp. 75–102, 2006.
- [12] —, "The CMA evolution strategy: A tutorial," *Vu le*, pp. 1–34, 2011. [Online]. Available: <http://www.lri.fr/~hansen/cmatutorial110628.pdf>
- [13] J. B. Andersen, C. Sternberg, L. K. Poulsen, S. P. Bjørn, M. Givskov, and S. r. Molin, "New unstable variants of green fluorescent protein for studies of transient gene expression in bacteria," *Applied and Environmental Microbiology*, vol. 64, no. 6, pp. 2240–2246, 1998.
- [14] R. Iizuka, M. Yamagishi-Shirasaki, and T. Funatsu, "Kinetic study of de novo chromophore maturation of fluorescent proteins," *Analytical Biochemistry*, vol. 414, no. 2, pp. 173–178, 2011. [Online]. Available: <http://dx.doi.org/10.1016/j.ab.2011.03.036>
- [15] G. L. Hersch, T. a. Baker, and R. T. Sauer, "SspB delivery of substrates for ClpXP proteolysis probed by the design of improved degradation tags," *Proceedings of the National Academy of Sciences of the United States of America*, vol. 101, no. 33, pp. 12 136–12 141, 2004.

## APPENDIX

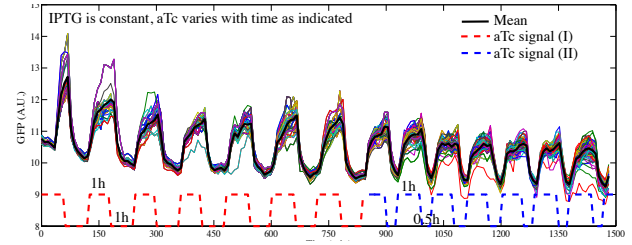


Fig. 5. A network with an intuitively clear community structure, which is captured by the partition chosen, shown in gray. Image reproduced from [3]

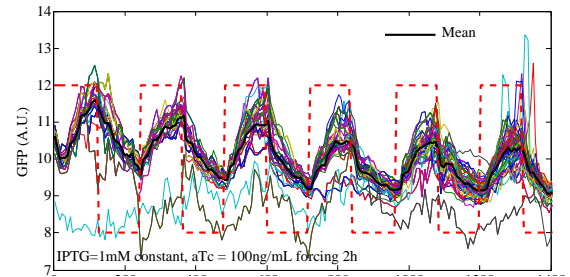


Fig. 6. A network with an intuitively clear community structure, which is captured by the partition chosen, shown in gray. Image reproduced from [3]

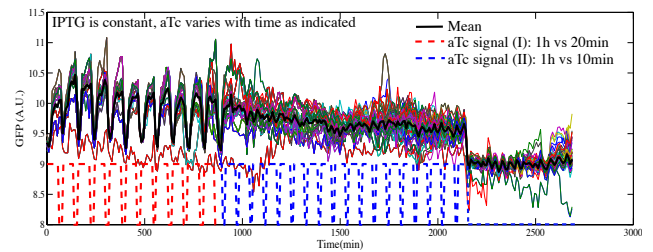


Fig. 7. A network with an intuitively clear community structure, which is captured by the partition chosen, shown in gray. Image reproduced from [3]



TABLE III. MODEL PARAMETERS

Parameter	Value	Definition	Reference	Initial Bounds
$N$	300	Number of copies of promoter existing on plasmid DNA	Experimentally set	
$z_0$	9 AFU	Baseline experimental fluorescence	Experimentally determined	
$\alpha_L$	11 nM/min	Maximal transcription rate of $P_{LlacO-1}$ promoter	[6]	
$\alpha_T$	11 nM/min	Maximal transcription rate of $P_{LtetO-1}$ promoter	[6]	
$f_L$	620	Unitless ratio between repressed and unrepressed $P_{LlacO-1}$ transcription rate	[6]	
$f_T$	2535	Unitless ratio between repressed and unrepressed $P_{LtetO-1}$ transcription rate	[6]	
$\delta_g$	0.0005 /min	GFP degradation rate	[13]	
$\gamma$	0.132 /min	GFP maturation rate	[14]	
$v_z$	100 nM/min	degradation constant of clpx	[15]	
$K_z$	75 nM/min	Dissociation constant of clpx	[15]	
$\Theta$	nM/AFU	Ratio between GFP concentration and observed fluorescence		300 - 1000
$\mu$	/min	Dilution rate		0.001-0.05
$\delta_m$	/min	mRNA degradation rate		1 - $10^5$
$\delta_s$	/min	sRNA degradation rate		1 - $10^3$
$\delta_{sm}$	/min	Unstable sRNA:mRNA degradation rate		Set to $\delta_m$
$\delta_c$	/min	Stable sRNA:mRNA degradation rate		Set to $\delta_m$
$k_{on}$	/min	sRNA:mRNA binding rate		100 - $10^7$
$k_{off}$	/min	sRNA:mRNA unbinding rate		1 - $10^8$
$k_{hyb}$	/min	sRNA:mRNA hybridization rate		1 - $10^4$
$\beta$	/min	Baseline translation rate of repressed mRNA		0.0001 - 10
$f_s$		Ratio of repressed mRNA to unrepressed complex translation rate.		0.1 - $10^4$